Advanced Functional Materials

Euryale Ferox Seed-inspired Super-lubricated Nanoparticles for Treatment of Osteoarthritis

--Manuscript Draft--

Manuscript Number:	adfm.201807559R1
Full Title:	Euryale Ferox Seed-inspired Super-lubricated Nanoparticles for Treatment of Osteoarthritis
Article Type:	Full Paper
Section/Category:	
Keywords:	Bioinspired; osteoarthritis; photopolymerization; lubrication; nanoparticles
Corresponding Author:	Helder Santos, D.Sc. (Chem. Eng.) University of Helsinki Helsinki, Helsinki FINLAND
Additional Information:	
Question	**Response**
Please submit a plain text version of your cover letter here.	Helsinki, 18 November 2018, Dr. Joern Ritterbusch Editor Advanced Functional Materials Dear Dr. Ritterbusch, I am submitting our revised manuscript (Full Paper, No. adfm.201807559) entitled "Euryale Ferox Seed-inspired Super-lubricated Nanoparticles for Treatment of Osteoarthritis" for publication as a full paper in Advanced Functional Materials. I would like first to thank You and the reviewers very much for the very positive and constructive comments for the improvement of our article, and for the possibility given to reply to the reviewers' comments. Based on the reviewers' comments (minor revisions), we have modified the revised manuscript accordingly to address all the comments. Please, find enclosed the replies to the reviewers' reports, which also summarize the changes made in the manuscript, highlighted in yellow. I believe that the changes introduced to the manuscript have further improved it and I hope that the manuscript can now be accepted for publication in your valuable journal. All authors have approved the manuscript and this submission. We thank you in advance for considering our work and look forward to hear from you in the near future. Please do not hesitate to contact me if you require any further information. Sincerely yours, Hélder Santos (corresponding author, on behalf of all co-authors)

	Hélder A. Santos, D.Sc. (Chem. Eng.), Associate Professor (Pharm. Nanotechnol.) Head of the Division of Pharmaceutical Chemistry and Technology Head of the Nanomedicines and Biomedical Engineering Group Head of the Preclinical Drug Formulation and Analysis Group Director of Doctoral Programme in Drug Research, University of Helsinki Drug Research Program, Faculty of Pharmacy, University of Helsinki, Finland & Helsinki Institute of Life Science (HiLIFE), University of Helsinki, Finland @: helder.santos@helsinki.fi http://www.helsinki.fi/~hsantos/
Do you or any of your co-authors have a conflict of interest to declare?	No. The authors declare no conflict of interest.
Corresponding Author Secondary Information:	
Corresponding Author's Institution:	University of Helsinki
Corresponding Author's Secondary Institution:	
First Author:	Yufei Yan
First Author Secondary Information:	
Order of Authors:	Yufei Yan
	Tao Sun
	Hongbo Zhang
	Xiuling Ji
	Yulong Sun
	Xin Zhao
	Lianfu Deng
	Jin Qi
	Wenguo Cui
	Helder Santos, D.Sc. (Chem. Eng.)
	Hongyu Zhang
Order of Authors Secondary Information:	
Abstract:	Osteoarthritis has been regarded as a typical lubrication deficiency related joint disease, which is characterized by the breakdown of articular cartilage at the joint surface and the inflammation of the joint capsule. Here, inspired by the structure of fresh euryale ferox seed that possesses a slippery aril and a hard coat containing starchy kernel, we biomimicked and synthesized a novel super-lubricated nanoparticle, namely poly (3-sulfopropyl methacrylate potassium salt)-grafted mesoporous silica nanoparticles (MSNs-NH2@PSPMK), via one-step photopolymerization method. The nanoparticles were endowed with enhanced lubrication by the grafted PSPMK polyelectrolyte polymer due to the formation of tenacious hydration layers surrounding the negative charges, and simultaneously were featured with effective drug loading and release behavior as a result of the sufficient mesoporous channels in the MSNs. When encapsulated with an anti-inflammatory drug diclofenac sodium (DS), the lubrication capability of the super-lubricated nanoparticles was improved, while the drug release rate was sustained by increasing the thickness of PSPMK layer, which

	was simply achieved via adjustment of the precursor monomer concentration in the photopolymerization process. Additionally, the in vitro and in vivo experimental results showed that the DS-loaded MSNs-NH2@PSPMK nanoparticles effectively protected the chondrocytes from degeneration, and thus, inhibited the development of osteoarthritis.

DOI: 10.1002/((please add manuscript number))
Article type: Article

Euryale Ferox Seed-inspired Super-lubricated Nanoparticles for Treatment of Osteoarthritis

Yufei Yan, Tao Sun, Hongbo Zhang, Xiuling Ji, Yulong Sun, Xin Zhao, Lianfu Deng, Jin Qi*, Wenguo Cui*, Hélder A. Santos*, Hongyu Zhang*

Dr. Y. Yan, Prof. L. Deng, J. Qi and Prof. W. Cui
Shanghai Key Laboratory for Prevention and Treatment of Bone and Joint Diseases, Shanghai Institute of Traumatology and Orthopaedics, Ruijin Hospital, Shanghai Jiao Tong University School of Medicine, Shanghai 200025, China.
Email: jinjin838@hotmail.com; wgcui80@hotmail.com
T. Sun, Dr. X. Ji, Y. Sun and Prof. H. Zhang
State Key Laboratory of Tribology, Department of Mechanical Engineering, Tsinghua University, Beijing 100084, China.
Email: zhanghyu@tsinghua.edu.cn
Prof. H. Zhang
Department of Pharmaceutical Sciences Laboratory, Åbo Akademi University, 20520 Turku, Finland.
Turku Center for Biotechnology, University of Turku and Åbo Akademi University, 20520 Turku, Finland.
Prof. X. Zhao
Department of Biomedical Engineering, The Hong Kong Polytechnic University, Hung Hom, Hong Kong, China.
Prof. H. A. Santos
Drug Research Program, Division of Pharmaceutical Chemistry and Technology, Faculty of Pharmacy, University of Helsinki, Helsinki FI-00014, Finland.
Email: helder.santos@helsinki.fi
Prof. H. A. Santos
Helsinki Institute of Life Science (HiLIFE), University of Helsinki, Helsinki FI-00014, Finland.

Abstract

Osteoarthritis has been regarded as a typical lubrication deficiency related joint disease, which is characterized by the breakdown of articular cartilage at the joint surface and the inflammation of the joint capsule. Here, inspired by the structure of fresh *euryale ferox* seed that possesses a slippery aril and a hard coat containing starchy kernel, we biomimicked and synthesized a novel super-lubricated nanoparticle, namely poly (3-sulfopropyl methacrylate potassium salt)-grafted mesoporous silica nanoparticles (MSNs-NH_2@PSPMK), via one-step photopolymerization method. The nanoparticles were endowed with enhanced lubrication by the grafted PSPMK polyelectrolyte polymer due to the formation of tenacious hydration layers surrounding the negative charges, and simultaneously were featured with effective drug loading and release behavior as a result of the sufficient mesoporous channels in the MSNs. When encapsulated with an anti-inflammatory drug diclofenac sodium (DS), the lubrication capability of the super-lubricated nanoparticles was improved, while the drug release rate was sustained by increasing the thickness of PSPMK layer, which was simply achieved via adjustment of the precursor monomer concentration in the photopolymerization process. Additionally, the *in vitro* and *in vivo* experimental results showed that the DS-loaded MSNs-NH_2@PSPMK nanoparticles effectively protected the chondrocytes from degeneration, and thus, inhibited the development of osteoarthritis.

Keywords: Bioinspired; osteoarthritis; photopolymerization; lubrication; nanoparticles.

1. Introduction

From an engineering point of view, osteoarthritis has been regarded as a lubrication deficiency related joint disease triggered by breakdown of articular cartilage and inflammation of the joint, and it is considered that a synergetic therapy combining both lubrication and drug intervention predicts a promising non-surgical strategy for treatment of osteoarthritis.[1,2] *Euryale ferox,* also known as foxnut or makhana, is a flowering plant classified in the family of Nymphaeaceae. The fresh *euryale ferox* seed is composed of a membranous aril outside and a hard coat inside containing starchy kernel.[3,4] The streaked bright red membranous aril is very slippery and slimy in nature, while the hard coat loads the starchy kernel which can be used for the treatment of articular joint pain. Accordingly, on the basis of inspiration from the structure of fresh *euryale ferox* seed, biomimetic nanoparticles may provide superlubricity on the outer surface and simultaneously drug loading in the inner core. Moreover, an intra-articular injection of such super-lubricated drug-loaded nanoparticles into the joint can achieve both lubrication improvement during joint movement and drug intervene via local administration, and thus, be served as an effective treatment for osteoarthritis.

Mesoporous silica nanoparticles (MSNs) have long been recognized to be representative drug nanocarriers, owing to their large surface area, large pore volume, high thermal stability and good biocompatibility.[5-9] Incorporating super-lubricated polymers onto the MSNs surface has been attempted as one of the most efficient and convenient approaches to construct multi-functional drug delivery systems with the feature of lubrication capability.[10] Various surface-grafted MSNs have been successfully developed for example, by different polymers via atom transfer radical polymerization,[11,12] reversible addition-fragmentation chain transfer polymerization,[13,14] and ring opening polymerization.[15] However, these methods can introduce toxic catalysts during the reaction, for example, the toxic metallic components in the process of atom transfer radical polymerization.[16] The toxic substances are difficult to be completely eliminated through post-processing, consequently limiting the biological applications of such polymer-grafted MSNs. Additionally, so far few studies have investigated the lubrication capability of polymer-grafted MSNs and their biological applications where enhanced lubrication and sustained drug delivery are preferably desirable, e.g., treatment of osteoarthritis. Therefore, developing super-lubricated drug-loaded MSNs without the involvement of complex synthesis and even the introduction of toxic catalysts is highly required but still remains a great challenge as yet.

Recently, hydration lubrication mechanism proposed by Klein et al. has been accepted to dominate the scenario of the excellent superlubricity for articular cartilage.[17,18] Particularly, it is considered that the hydration layers surrounding both the positive ($N^+(CH_3)_3$) and negative (PO_4^-) charges of the zwitterionic headgroups in the phosphatidylcholine lipids can bear typical joint pressures (4~10 MPa) with the friction coefficient at the joint interface at a level as low as 0.001~0.01. This is because the water molecules within the hydration layers are tenaciously held due to the interaction of the large water dipole with the enclosed charge, and will respond in a fluidlike manner when being sheared.[19,20] Furthermore, various polyelectrolyte polymer brushes used to mimic the biomolecules of articular cartilage have been proved to significantly reduce friction coefficient based on the hydration lubrication mechanism.[21-23] Accordingly, in view of the excellent superlubricity behavior of the articular cartilage, grafting polyelectrolyte polymer brushes onto the MSNs surface may represent an effective approach to endow MSNs with enhanced lubrication capability.

In the present study, inspired by the unique structure of fresh euryale ferox seed which consists of a slippery aril outside and a starchy kernel-loaded hard coat inside, we develop a facile and low-toxic photopolymerization method to synthesize super-lubricated drug-loaded MSNs. As demonstrated in Scheme 1a, the slippery aril corresponds to the super-lubricated polyelectrolyte polymer brushes, poly (3-sulfopropyl methacrylate potassium salt) (PSPMK), and the starchy kernel-loaded hard coat corresponds to the diclofenac sodium (DS)-loaded nanocarriers (MSNs-NH_2@DS). We hypothesize that the super-lubricated drug-loaded MSNs developed here, MSNs-NH_2@PSPMK-DS, can be used as an effective intra-articular injective agent to inhibit the development of osteoarthritis, as shown in Scheme 1b.

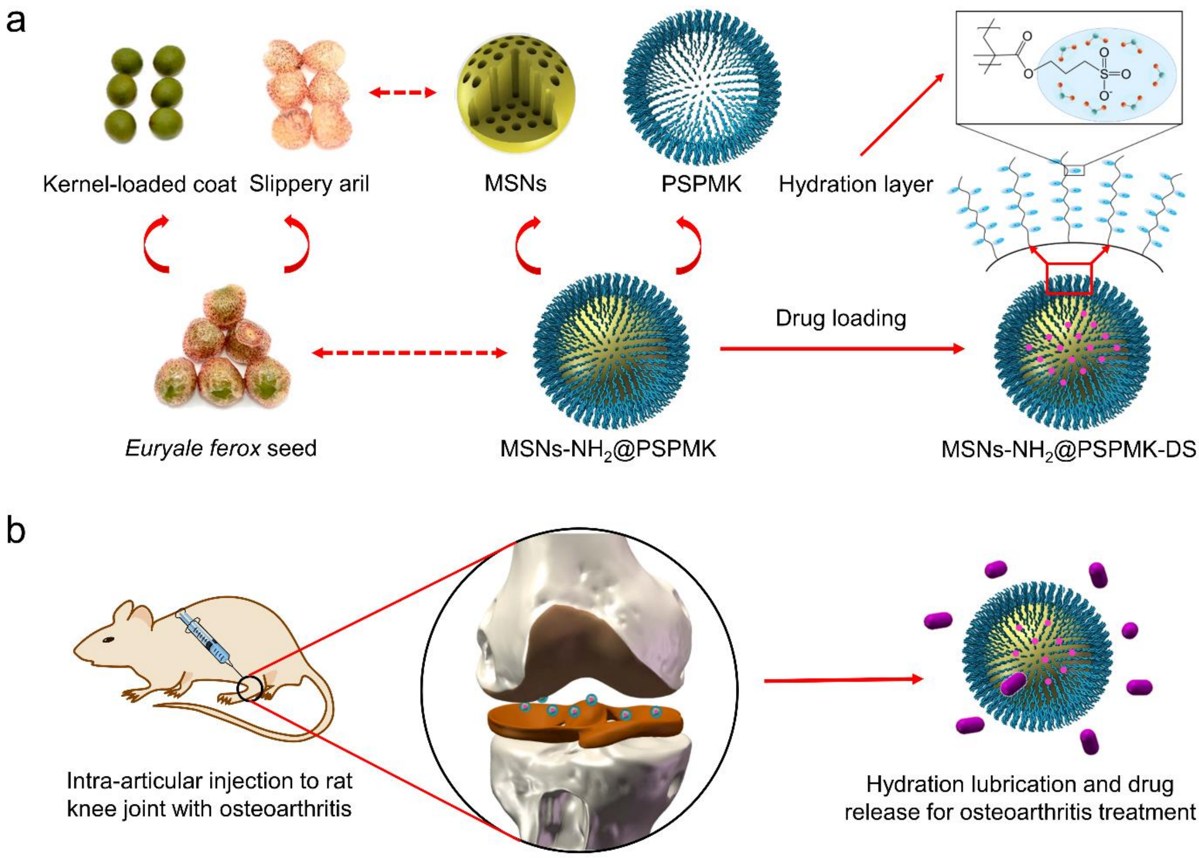

Scheme 1. Schematic illustration showing (a) the design of the super-lubricated drug-loaded nanoparticles, MSNs-NH_2@PSPMK-DS, which is bioinspired by the structure of fresh *euryale ferox* seed, and (b) the *in vitro* and *in vivo* experiments, showing the treatment of osteoarthritis by MSNs-NH_2@PSPMK-DS based on synergetic effect of enhanced lubrication and sustained drug release.

2. Results and Discussion

We biomimicked and synthesized super-lubricated drug-loaded MSNs, MSNs-NH_2@PSPMK-DS, for the treatment of osteoarthritis. For this we first prepared super-lubricated nanoparticles, PSPMK-grafted MSNs (MSNs-NH_2@PSPMK), by grafting SPMK monomer onto the surface of MSNs via photopolymerization, employing 2959-Tos as the initiator. Briefly, 2959-Tos was immobilized onto the surface of MSNs, and the resulting product (MSNs-NH_2@I2959) was uniformly dispersed in SPMK monomer solution and reacted under UV-irradiation to obtain MSNs-NH_2@PSPMK. Subsequently, MSNs-NH_2@PSPMK were encapsulated with DS, a widely used nonsteroidal anti-inflammatory drug in clinics, to prepare MSNs-NH_2@PSPMK-DS as a novel super-lubricated drug-loaded nanoparticle. Similar to fresh *euryale ferox* seed, the polymer layer of MSNs-NH_2@PSPMK-DS corresponding to the slippery aril was expected to endow the nanoparticles with lubrication capability, while DS-loaded MSNs corresponding to the starchy kernel-loaded hard coat to endow the nanoparticles with sustained drug release. The lubrication capability and drug release behavior of the nanoparticles can be easily tuned through controlling the thickness of the PSPMK layer by adjusting the monomer concentration in the photopolymerization process.

2.1. Characterization of Super-lubricated Nanoparticles

Fourier transform infrared (FTIR) spectroscopy analysis was conducted to investigate the successful surface grafting reaction. As shown in Figure 1a, the spectra of MSNs, MSNs-NH_2@I2959, and MSNs-NH_2@PSPMK (0.500 M SPMK) all demonstrate the absorption band of Si-O-Si at 1093 cm^{-1} and the stretching vibration of Si-OH at 3439 cm^{-1}. Compared with MSNs, only slight differences are observed in the spectrum of MSNs-NH_2@I2959, as the amount of photopolymerization initiator 2959-Tos modified on the MSNs surface is small. After the PSPMK polymer is grafted on the surface of MSNs, the absorption bands of S=O in SO_3^- appear at 1045 cm^{-1} and 1190 cm^{-1}, and the absorption band of C=O appears at 1720 cm^{-1}, as demonstrated from the spectrum of MSNs-NH_2@PSPMK. The presence of these absorption bands confirms that PSPMK polyelectrolyte polymer has been successfully grafted on the MSNs surface via photopolymerization.

Surface compositions of MSNs, MSNs-NH_2@I2959 and MSNs-NH_2@PSPMK (0.500 M SPMK) were also evaluated by X-ray photoelectron spectroscopy (XPS). As shown in Figure 1b, for MSNs, the binding energies of Si 2p and Si 2s are at 104 eV and 155 eV, respectively. For MSNs-NH_2@I2959, the signal of N 1s at 398 eV is attributed to the introduction of amine groups on the MSNs surface. For MSNs-NH_2@PSPMK, the grafting of the PSPMK polymer on the MSNs surface is confirmed by the signals of K and S elements appearing at 377 eV (K 2s), 293 eV (K 2p), 232 eV (S 2s) and 168 eV (S 2p).

Surface morphologies of MSNs and MSNs-NH_2@PSPMK were observed using transmission electron microscopy (TEM). Figure 1c (i) shows that MSNs have well-organized lattices, with an average diameter of about 114 nm. Figure 1c (ii-iv) demonstrates MSNs-NH_2@PSPMK prepared by photopolymerization with different SPMK monomer concentrations. It is evident that all the MSNs-NH_2@PSPMK nanoparticles are surrounded by a shaded polymer layer, and the thickness of the polymer layer is ~4 nm for MSNs-NH_2@PSPMK-0.125, 7 nm for MSNs-NH_2@PSPMK-0.250 and 9 nm for MSNs-NH_2@PSPMK-0.500, respectively, which indicates that there is a positive correlation between the SPMK monomer concentration and the polymer layer thickness.

Figure 1d exhibits the thermogravimetric analysis (TGA) results obtained for MSNs, MSNs-NH_2, MSNs-NH_2@I2959 and MSNs-NH_2@PSPMK. To eliminate the interference from bound water on the surface of MSNs, the data are organized with the temperature starting from 100 °C. After amination and immobilization of the initiator, a weight loss of 12.9% and 14.2% is observed, through which the content of the initiator is calculated to be 1.5%. When the PSPMK polymer is grafted on the MSNs surface, the weight losses increase to 27.9% for MSNs-NH_2@PSPMK-0.125, 29.1% for MSNs-NH_2@PSPMK-0.250 and 38.0% for MSNs-NH_2@PSPMK-0.500, respectively. As a result, the contents of the PSPMK polymer are calculated to be 16.0%, 17.4% and 27.7%, respectively. The TGA data not only confirm the successful grafting of PSPMK polyelectrolyte polymer on the MSNs surface, but also provide a quantitative evaluation for each component of the nanoparticles, as summarized in Table 1. It can be observed that with increasing SPMK monomer concentration, the amount of the PSPMK polyelectrolyte polymer grafted on the MSNs surface increases remarkably.

Table 1. The weight ratio of each component in MSNs-NH_2@I2959 and MSNs-NH_2@PSPMK calculated from TGA data.

	MSNs-NH_2	Irgacure 2959	PSPMK
MSNs-NH_2@I2959	98.5%	1.5%	
MSNs-NH_2@PSPMK-0.125	82.7%	1.3%	16.0%
MSNs-NH_2@PSPMK-0.250	81.4%	1.2%	17.4%
MSNs-NH_2@PSPMK-0.500	71.2%	1.1%	27.7%

In order to further investigate the pore properties of MSNs and MSNs-NH_2@PSPMK, the N_2 adsorption-desorption isotherms of the nanoparticles were measured. As shown in Figure 1e, all the isotherms demonstrate typical type IV N_2 adsorption/desorption patterns, indicating a mesoporous structure of the nanoparticles. Based on the Brunauer-Emmett-Teller (BET) model, the specific surface area and pore volume of MSNs are calculated to be 805 m^2/g and 0.806 mL/g. Following grafting of PSPMK polyelectrolyte polymer on the MSNs surface, both specific surface area and pore volume of the nanoparticles decrease significantly, i.e., 429.6 m^2/g and 1.20 mL/g for MSNs-NH_2@PSPMK-0.125, 299.1 m^2/g and 1.11 mL/g for MSNs-NH_2@PSPMK-0.250 and 23.6 m^2/g and 0.09 mL/g for MSNs-NH_2@PSPMK-0.500, respectively. This result indicates that the mesoporous channels have been blocked by the PSPMK polyelectrolyte polymer.

Figure 1f displays the small-angle X-ray diffraction (XRD) patterns of MSNs and MSNs-NH_2@PSPMK, showing the microcrystalline of the nanoparticles. The presence of the standard Bragg peaks of (100), (110) and (200) indicates the highly ordered hexagonal array of MSNs. After the MSNs surface is grafted with PSPMK polyelectrolyte polymer, the Bragg peaks of (110) and (200) almost disappear for all of the MSNs-NH_2@PSPMK nanoparticles, which is mainly due to the weak crystallinity of PSPMK polyelectrolyte polymer.

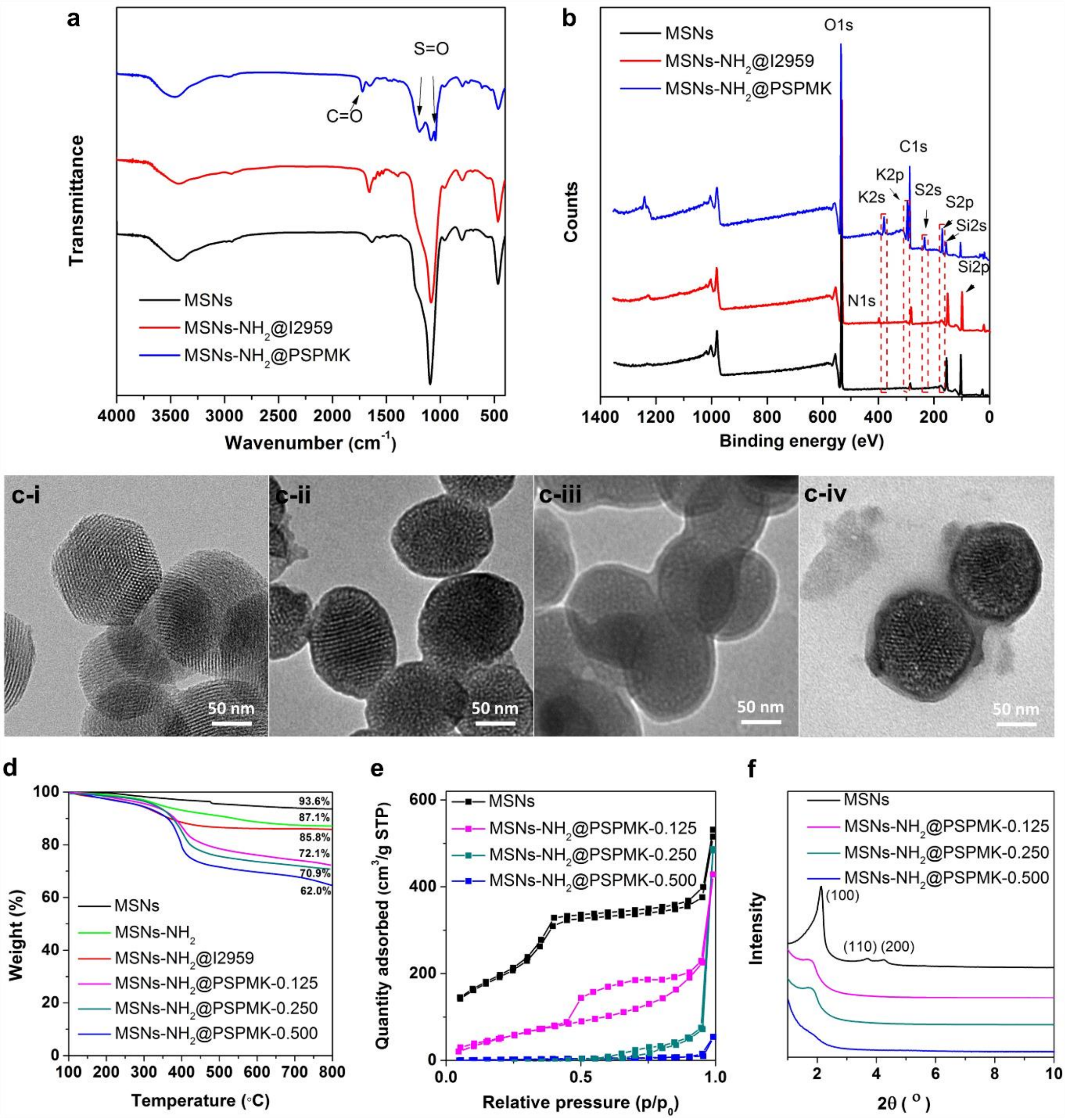

Figure 1. (a) FTIR spectra and (b) XPS spectra of MSNs, MSNs-NH_2@I2959 and MSNs-NH_2@PSPMK. (c) The TEM images of MSNs and MSNs-NH_2@PSPMK with three different SPMK monomer concentrations: (c-i) MSNs; (c-ii) MSNs-NH_2@PSPMK-0.125;

(c-iii) MSNs-NH_2@PSPMK-0.250; (c-iv) MSNs-NH_2@PSPMK-0.500. The thickness of the polymer layer is ~4 nm, 7 nm and 9 nm, respectively. (d) TGA curves, (e) N_2 adsorption-desorption isotherm curves and (f) Small-angle XRD patterns of MSNs and MSNs-NH_2@PSPMK with three different SPMK monomer concentrations.

2.2. Super-lubricated Property and Analysis

The tribological experiment was performed to investigate the lubrication property of MSNs and MSNs-NH_2@PSPMK in aqueous suspension. As shown from the friction coefficient-time plots in Figure 2a (i) (loading force: 5N; reciprocating frequency: 3 Hz; concentration: 5 mg mL^{-1}), the friction coefficient of MSNs is 0.168, which is much higher than that of MSNs-NH_2@PSPMK with different monomer concentrations. Additionally, it is observed that as the monomer concentration increases, the friction coefficient value reduces gradually, i.e., 0.145 for MSNs-NH_2@PSPMK-0.125, 0.102 for MSNs-NH_2@PSPMK-0.250 and 0.065 for MSNs-NH_2@PSPMK-0.500, respectively. Figure 2a (ii) shows the comparison of friction coefficient lubricated using MSNs and MSNs-NH_2@PSPMK at different aqueous suspension concentrations (1 mg mL^{-1}, 2 mg mL^{-1} and 5 mg mL^{-1}) under the reciprocating frequency of 3 Hz and the loading force of 5 N. It is observed that all the friction coefficients of MSNs-NH_2@PSPMK are lower than that of MSNs, and generally the lubrication is improved with the increase in aqueous suspension concentration. Figure 2a (iii) demonstrates the comparison of friction coefficient lubricated by MSNs and MSNs-NH_2@PSPMK at different reciprocating frequencies (1 Hz, 3 Hz and 5 Hz) under the loading force of 5 N and the aqueous suspension concentration of 5 mg mL^{-1}. The friction coefficients are relatively small, and there seems to be a decreasing trend with the increase in reciprocating frequency although the difference between 3 Hz and 5 Hz is slight. Figure 2a (iv) presents the comparison of friction coefficient lubricated by MSNs and MSNs-NH_2@PSPMK at different loading forces (1 N, 2 N and 5 N) under the reciprocating frequency of 3 Hz and the aqueous suspension concentration of 5 mg mL^{-1}. The friction coefficients remain at a low level, and there seems to be a decreasing trend with the increase in loading force. The results indicate that the charged polymer covering the surface of MSNs-NH_2@PSPMK can achieve improved lubrication based on hydration lubrication mechanism,[24] which is mainly caused by the formation of hydration layers surrounding the negative charges of PSPMK polyelectrolyte polymer.

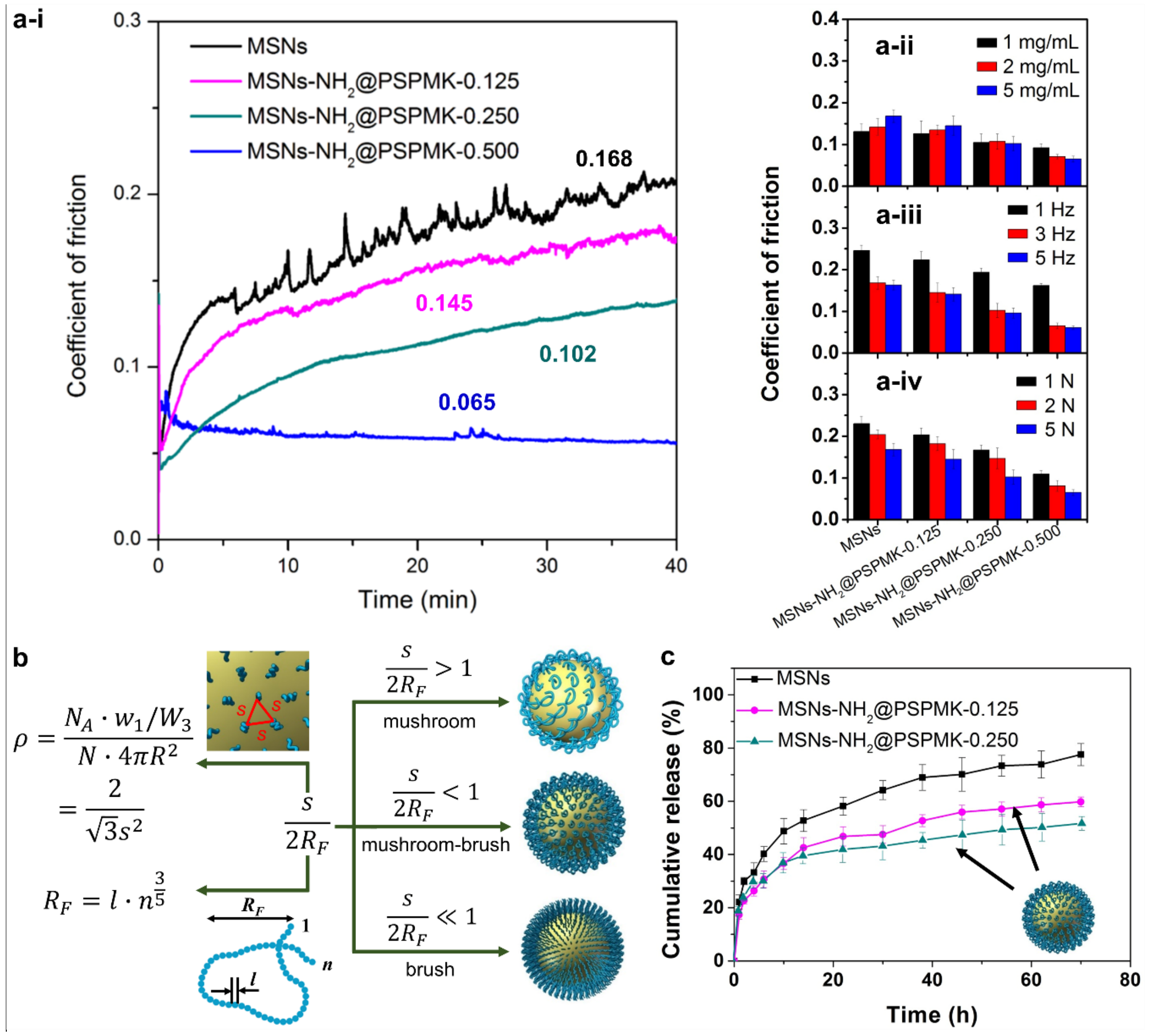

Figure 2. (a-i) The lubrication property of MSNs and MSNs-NH_2@PSPMK nanoparticles in aqueous suspension. Contacting pairs: Ti6Al4V disk and PE ball; duration: 40 min; oscillation amplitude: 4 mm; (a-ii) aqueous suspension concentration: 1 mg mL^{-1}, 2 mg mL^{-1} and 5 mg mL^{-1}; (a-iii) reciprocating frequency: 1 Hz, 3 Hz and 5 Hz; (a-iv) loading force: 1 N, 2 N and 5 N. (b) Schematic graph showing the calculation of different configurations of PSPMK polymer chains on the MSNs surface. The polymer chains are in the "mushroom-brush" state for MSNs-NH_2@PSPMK-0.125 and MSNs-NH_2@PSPMK-0.250, and they are in the "brush" state for MSNs-NH_2@PSPMK-0.500. (c) Release profiles of DS-loaded MSNs and DS-loaded MSNs-NH_2@PSPMK nanoparticles in PBS at 37 °C for 72

h. A sustained drug release profile is observed for MSNs-NH_2@PSPMK-0.125 and MSNs-NH2@PSPMK-0.250.

Figure 2a shows that the lubrication performance of MSNs-NH_2@PSPMK improves significantly along with thicker PSPMK polymer layer on the MSNs surface. This phenomenon may be due to the different configurations of the PSPMK polymer chains, which exhibit three potential states, namely “mushroom” state (the polymer chains are aggregated), “mushroom-brush” state (the polymer chains are stretched incompletely) and “brush” state (the polymer chains are stretched completely) (Figure 2b), depending on the ratio of the average distance between the PSPMK polymer chains (s) and the Flory radius (R_F).[25,26] Generally, in case that s is larger than $2R_F$, PSPMK polymer chains are in the “mushroom” state as a result of the free movement of polymer segments. If s is far less than $2R_F$, PSPMK polymer chains are in the “brush” state due to the repulsive force between the polymer chains. Besides, PSPMK polymer chains are in the “mushroom-brush” state. The values of s and R_F for MSNs-NH_2@PSPMK with different SPMK monomer concentrations are calculated and summarized in Table 2, and the calculation process is mentioned in detail in Supporting Information.

Table 2. Calculation of the parameters of PSPMK polymer chains for MSNs-NH_2@PSPMK with different monomer concentrations.

	n	R_F (nm)	s (nm)	$s/2R_F$
MSNs-NH_2@PSPMK-0.125	11.2	1.32		0.34
MSNs-NH_2@PSPMK-0.250	13.2	1.46	0.90	0.31
MSNs-NH_2@PSPMK-0.500	22.9	2.03		0.22

According to the previously published studies,[19,25] when $0.3 < s/2R_F < 1.2$, the polymer chains can be generally considered in the "mushroom-brush" state (e.g. MSNs-NH_2@PSPMK-0.125 and MSNs-NH_2@PSPMK-0.250), and when $s/2R_F < 0.3$, the polymer chains will be in the "brush" state (e.g. MSNs-NH_2@PSPMK-0.500). Figure 2a shows that the PSPMK polymer chains in the "mushroom-brush" state or "brush" state can result in a significant reduction in the friction coefficient. Additionally, the lubrication property of the PSPMK polymer chains in the "brush" state is even better than that in the "mushroom-brush" state, where the polymer chains are unable to be completely stretched out, and thus, hydration lubrication is to a certain degree compromised.

2.3. *In Vitro* Drug Loading and Release

The results of drug loading capacity (LC, %) and encapsulation efficiency (EE, %) of MSNs and MSNs-NH_2@PSPMK are shown in Table 3.

Table 3. Loading capacity (LC, %) and encapsulation efficiency (EE, %) of DS-loaded MSNs and DS-loaded MSNs-NH_2@PSPMK.

	LC (%)	EE (%)
MSNs	5.8	77.2
MSNs-NH_2@PSPMK-0.125	2.8	36.4
MSNs-NH_2@PSPMK-0.250	2.3	29.6
MSNs-NH_2@PSPMK-0.500	0.4	4.9

The PSPMK polyelectrolyte polymer on the MSNs surface impedes encapsulation of DS, and MSNs-NH_2@PSPMK-0.500 hardly adsorb any DS, indicating that the polymer layer is too thick for the drug molecules to penetrate through into the channels. Figure 2c presents the release profiles of DS-loaded MSNs and DS-loaded MSNs-NH_2@PSPMK. All the curves show an initial rapid drug release within 10 h, followed by a relatively flat stage afterward. When MSNs, MSNs-NH_2@PSPMK-0.125 and MSNs-NH_2@PSPMK-0.250 are used as the nanocarriers, 77.6%, 59.8% and 47.2% of DS are released within 72 h, respectively, demonstrating the excellent sustained release effect of MSNs-NH_2@PSPMK. It is noted that the release profile of MSNs-NH_2@PSPMK-0.500 is not provided due to the extremely low drug loading capacity.

From Table 3 it can be seen that the drug loading capacity of MSNs-NH_2@PSPMK decreases along with thicker PSPMK polymer layers on the MSNs surface. Additionally, from the drug release profiles of the three nanoparticles in Figure 2c, MSNs-NH_2@PSPMK-0.125 and MSNs-NH_2@PSPMK-0.250 exhibit a sustained drug release behavior, indicating that the hydrated PSPMK polymer chains on the MSNs surface are both penetrable and impeditive for the drug. It is considered that when the polymer chains are in the "mushroom-brush" state or the short-length "brush" state, MSNs-NH_2@PSPMK can be used as a nanocarrier for sustained drug release, until the length of the polymer chains increases and blocks drug loading into the mesoporous channels of the nanoparticles, e.g. in the case of MSNs-NH_2@PSPMK-0.500. In addition, the drug loading process of MSNs-NH_2@PSPMK, i.e., the preparation of DS-loaded MSNs-NH_2@PSPMK, is performed after surface grafting of PSPMK polyelectrolyte polymer on the MSNs surface. This is mainly because the drug may experience a rapid release during the photopolymerization process if it is initially loaded into MSNs. On the other hand, the UV-irradiation may cause potential influence on the drug activity, which as a consequence further affects the therapeutic effect of DS-loaded MSNs-NH_2@PSPMK for oxidative stress-induced degeneration of chondrocytes (*in vitro* test) and treatment of osteoarthritis (*in vivo* test).

2.4. *In Vitro* Cytotoxicity and Protective Effect of Chondrocytes Degeneration

In order to examine the potential clinical application of the developed super-lubricated drug-loaded nanoparticles, we investigated the *in vitro* cytotoxicity of MSNs, MSNs-NH_2@PSPMK and MSNs-NH_2@PSPMK-DS on primary rat chondrocytes, and subsequently performed experiments to indicate whether MSNs-NH_2@PSPMK-DS could protect the oxidative stress-induced degeneration of the chondrocytes. It was noted that MSNs-NH_2@PSPMK and MSNs-NH_2@PSPMK-DS used in the following tests were prepared with the SPMK monomer concentration of 0.250 M, as the nanoparticles made at this concentration demonstrated both good lubrication property and sustained drug release behavior.

The *in vitro* cytotoxicity of MSNs, MSNs-NH_2@PSPMK and MSNs-NH_2@PSPMK-DS on primary rat chondrocytes are first discussed. Following incubation at 1, 3 and 5 days, the cells were proceeded for CCK-8 test and Live/Dead assay. In Figure 3a the CCK-8 test shows that the cell viability and proliferation activity have no significant difference among the experimental groups compared with the control group at all time points. In addition, the Live/Dead staining show that most of the seeded cells stay alive and only very few dead cells are observed over the course of 5-day culture (Figure 3b). Furthermore, the cell density increased gradually with time from day 1 to day 5, which is confirmed by the data of the number of viable cells shown in Figure 3c. All these results indicate that the nanoparticles show excellent biocompatibility to the chondrocytes.

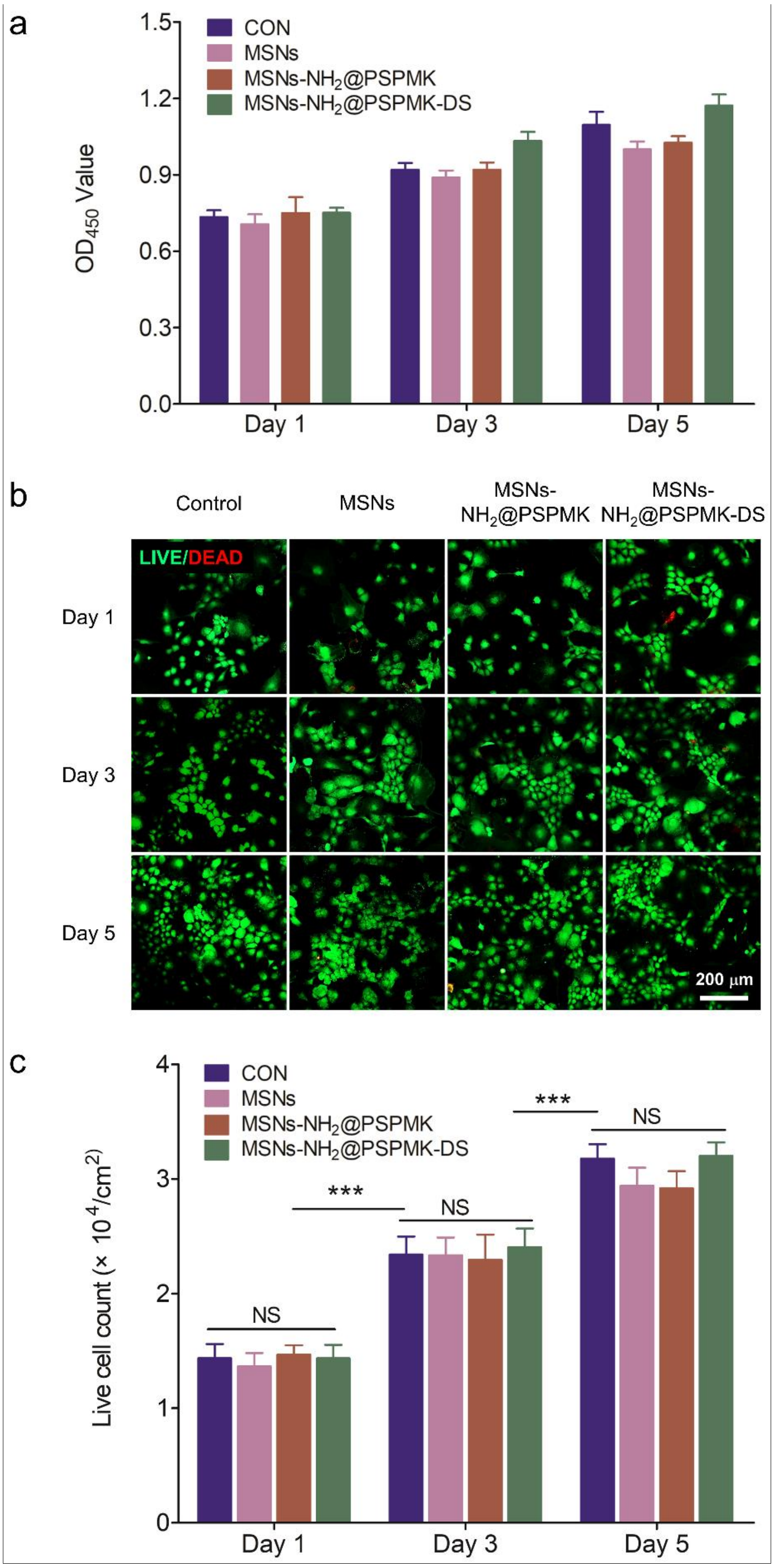

Figure 3. (a) Cytotoxicity of MSNs, MSNs-NH_2@PSPMK and MSNs-NH_2@PSPMK-DS on chondrocytes examined with CCK-8. (b) Live/Dead staining of chondrocytes co-cultured

with MSNs, $MSNs\text{-}NH_2$@PSPMK and $MSNs\text{-}NH_2$@PSPMK-DS detected employing fluorescence microscopy. All the nanoparticles show excellent biocompatibility to the chondrocytes. (c) The live cell count summarized from the Live/Dead assay. n=3; NS=no significance; ***$P < 0.001$.

Multiple factors are associated with pathogenesis of osteoarthritis, such as reactive oxygen species (ROS), mechanical loading stress, and inflammatory factors. These factors can result in chondrocytes degeneration, which is the most significant characteristic of osteoarthritis. In this study, we introduced H_2O_2 to simulate ROS stress of chondrocytes during the pathogenesis of osteoarthritis. The robust production of Col2α and aggrecan are important characteristics of healthy chondrocytes. After addition of H_2O_2, the mRNA expression of Col2α and aggrecan both decrease gradually with prolonged culture time and to less than half of the original value (0 h) at 12 h. Moreover, a significant reduction in the mRNA expression of Col2α and aggrecan is observed at 24 h after addition of H_2O_2 (Figure 4a and 4b). In order to explore the protective effect of $MSNs\text{-}NH_2$@PSPMK-DS for chondrocytes degeneration, subsequently we evaluated the mRNA expression of Col2α and aggrecan in chondrocytes after addition of MSNs, $MSNs\text{-}NH_2$@PSPMK and $MSNs\text{-}NH_2$@PSPMK-DS with H_2O_2. The qRT-PCR analyses indicate that the mRNA expression of Col2α and aggrecan increases significantly after addition of $MSNs\text{-}NH_2$@PSPMK-DS, whilst no significant changes have been observed for MSNs and $MSNs\text{-}NH_2$@PSPMK, which clearly indicates the protective effect of $MSNs\text{-}NH_2$@PSPMK-DS for chondrocytes degeneration (Figure 4c and 4d).

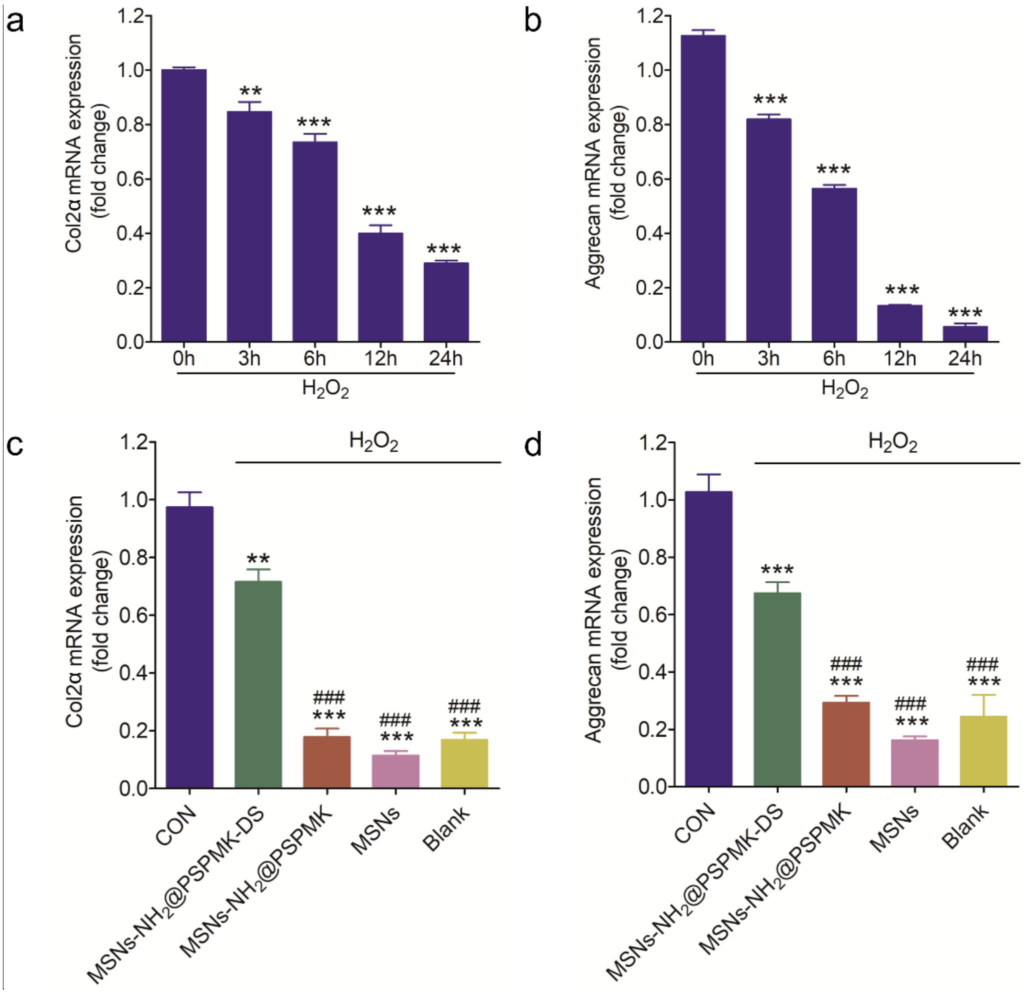

Figure 4. (a and b) The qRT-PCR analysis exhibiting the mRNA expression of Col2α (a) and aggrecan (b) in chondrocytes treated with 10 mU of H_2O_2 at deferent time points. n = 3, *P < 0.05, **P < 0.01, ***P < 0.001, compared with control (0 h). (c and d) The qRT-PCR analysis showing the mRNA expression of Col2α (c) and aggrecan (d) in chondrocytes treated with 10 mU of H_2O_2, and co-cultured with MSNs, MSNs-NH_2@PSPMK and MSNs-NH_2@PSPMK-DS for 24 h. n = 3, **P < 0.01, ***P < 0.001, compared with control; $^{###}$P < 0.001, compared with MSNs-NH_2@PSPMK-DS. The data clearly demonstrate the protective effect of MSNs-NH_2@PSPMK-DS for chondrocytes degeneration.

Furthermore, the result of immunofluorescence staining and corresponding statistical analysis show that the addition of MSNs-NH_2@PSPMK-DS can reverse H_2O_2 stress-induced reduction of Col2α protein expression compared with the MSNs and MSNs-NH_2@PSPMK groups (Figure 5). As a consequence, the results confirm the protective effect of MSNs-NH_2@PSPMK-DS for chondrocytes degeneration and tentatively suggest the potential clinical application for treatment of osteoarthritis.

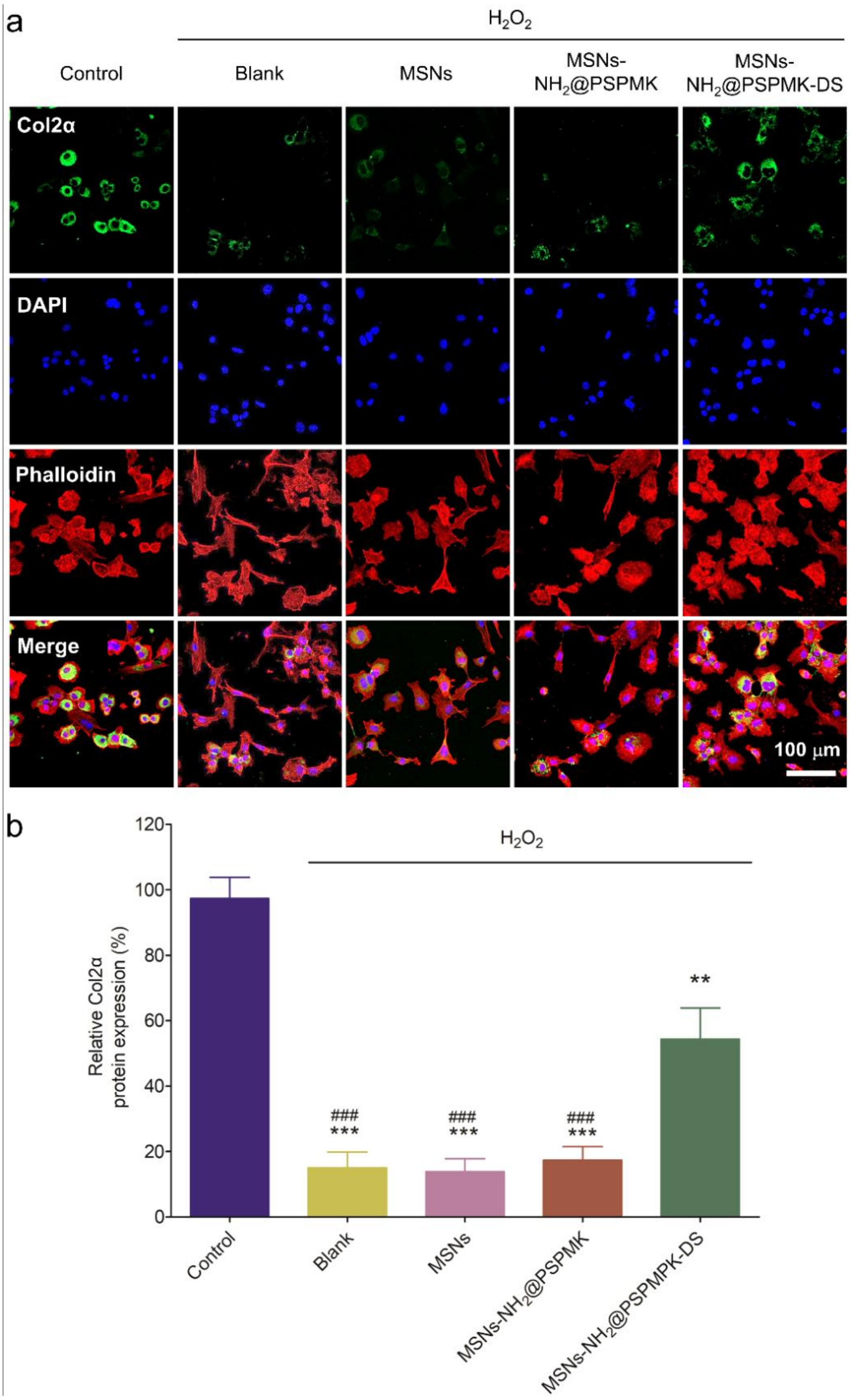

Figure 5. (a) Representative photomicrographs of chondrocytes treated with 10 mU of H_2O_2 and co-cultured with MSNs, MSNs-NH_2@PSPMK and MSNs-NH_2@PSPMK-DS for 12 h, acquired using a laser scanning confocal microscopy. Green: Molecular Probes labeling Col2α; Blue: DAPI labeling cell nuclei; Red: Phalloidin labeling cell actin. (b) The quantitative data showing comparison of Col2α protein expression of chondrocytes treated with 10 mU of H_2O_2, and co-cultured with MSNs, MSNs-NH_2@PSPMK and MSNs-NH_2@PSPMK-DS for 12 h. n = 3, $^{**}P < 0.01$, $^{***}P < 0.001$, compared with control; $^{\#\#\#}P < 0.001$, compared with MSNs-NH_2@PSPMK-DS. The results confirm the protective effect of MSNs-NH_2@PSPMK-DS for chondrocytes degeneration.

2.5. *In Vivo* Therapeutic Effect of Osteoarthritis

An animal model of destabilization of the medial meniscus (DMM)-induced osteoarthritis has been commonly employed in previous studies.[27] In the present study, we performed *in vivo* analysis of Sprague-Dawley rats that had undergone DMM surgery, including X-ray radiograph and histological staining. One week following the DMM surgery, the rats were injected once every week with PBS, MSNs, MSNs-NH_2@PSPMK and MSNs-NH_2@PSPMK-DS. Figure 6a shows the X-ray radiographs of the knee joints of the rats obtained at one and eight weeks after the DMM surgery, and no signs of acute inflammation are observed in any of these treatment groups (including MSNs, MSNs-NH_2@PSPMK and MSNs-NH_2@PSPMK-DS). In addition, the values of articular space width are calculated from the radiographies, and it is indicated that the medial compartments between femur and tibia become narrower at eight weeks after DMM surgery for all the groups, although it seems that the MSNs-NH_2@PSPMK-DS group generates a slightly larger articular space width, Figure 6b.

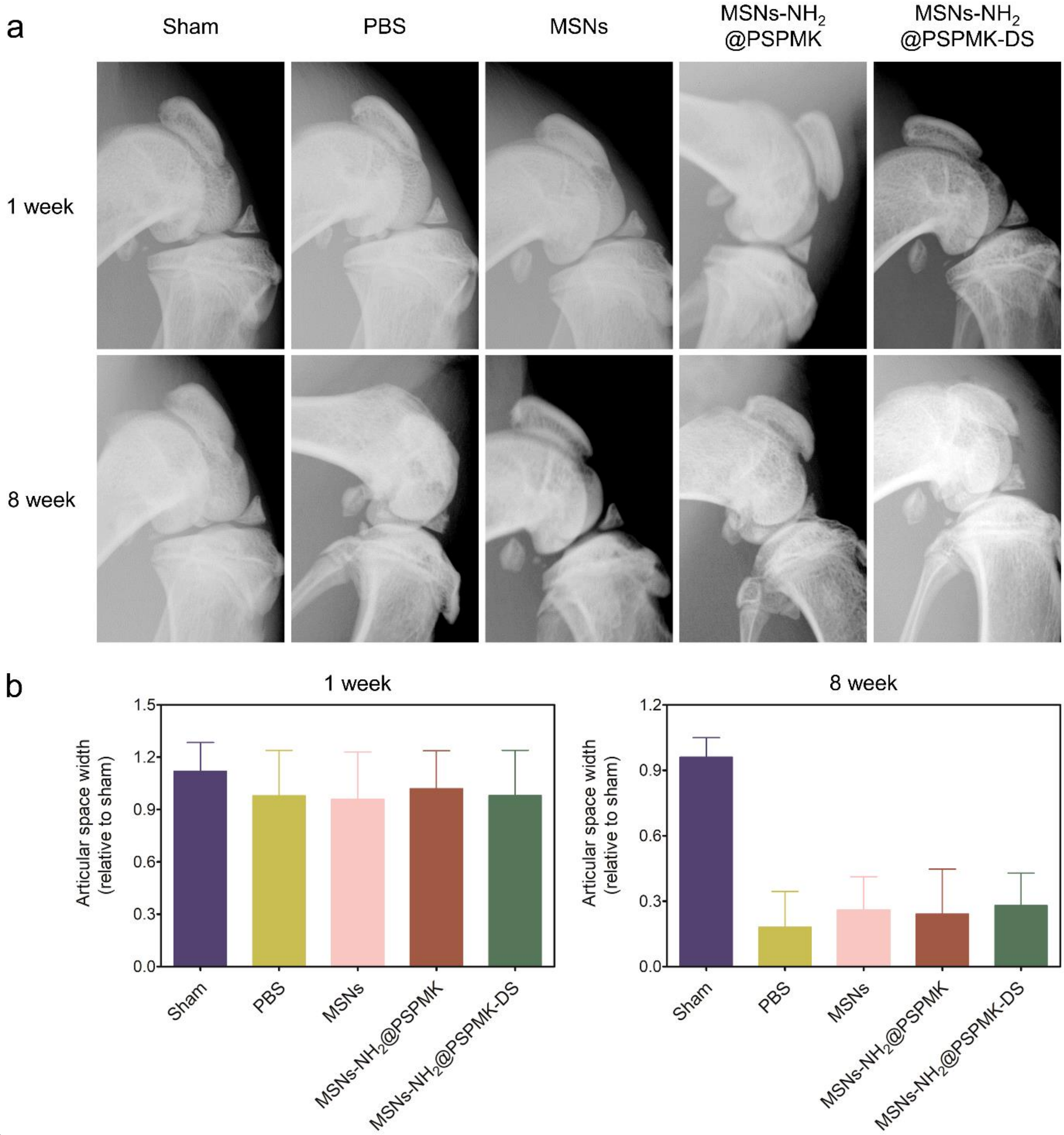

Figure 6. (a) Representative X-ray radiographs of the rat knee joints showing the intra-articular injection of PBS, MSNs, MSNs-NH_2@PSPMK and MSNs-NH_2@PSPMK-DS in the treatment of DMM-induced osteoarthritis at one and eight weeks after surgery. (b) The

relative articular space width between the medial compartments of rat knee joints at one and eight weeks after surgery. No signs of acute inflammation are observed from the X-ray radiographs of the MSNs, MSNs-NH_2@PSPMK and MSNs-NH_2@PSPMK-DS groups.

The cartilage tissues were then evaluated histologically by H&E staining and Safranin O-fast green staining. As displayed in Figure 7a and 7b, typical osteoarthritis features, such as surface discontinuity, vertical fissure, erosion denudation and deformation, are observed in the PBS group. Compared with the PBS group, all the treatment groups present varied degrees of improvement with respect to morphological change, matrix staining and tidemark integrity promotion. Specifically, the MSNs-NH_2@PSPMK-DS group is considered the most effective in maintaining the columnar architecture of normal cartilage, which is typically manifested as less severe lesion and extensive erosion, decreased surface denudation and deformation, as well as increased tissue cellularity and cloning. Furthermore, the MSNs-NH_2@PSPMK-DS group shows more intense Safranin O-fast green positive staining than do the other groups (Figure 7c). This finding indicates that the MSNs-NH_2@PSPMK-DS group has better outcome with respect to glycosaminoglycan deposition, attenuation of cartilage matrix depletion and also retention of overall cartilage thickness. The result of OARSI score is illustrated in Figure 7d. All the treatment groups decrease the OARSI score more or less compared with the PBS group, and the MSNs-NH_2@PSPMK-DS group shows the best result with about 64% reduction. In addition, the depth of the cartilage macroscopic lesion is also compared for each group at eight weeks after DMM surgery, and again the MSNs-NH_2@PSPMK-DS group demonstrates the best result with about 55% reduction relative to the PBS group (Figure 7e). All these results indicate that the super-lubricated drug nanocarrier (MSNs-NH_2@PSPMK-DS) can inhibit development of osteoarthritis based on the *in vivo* rat DMM model.

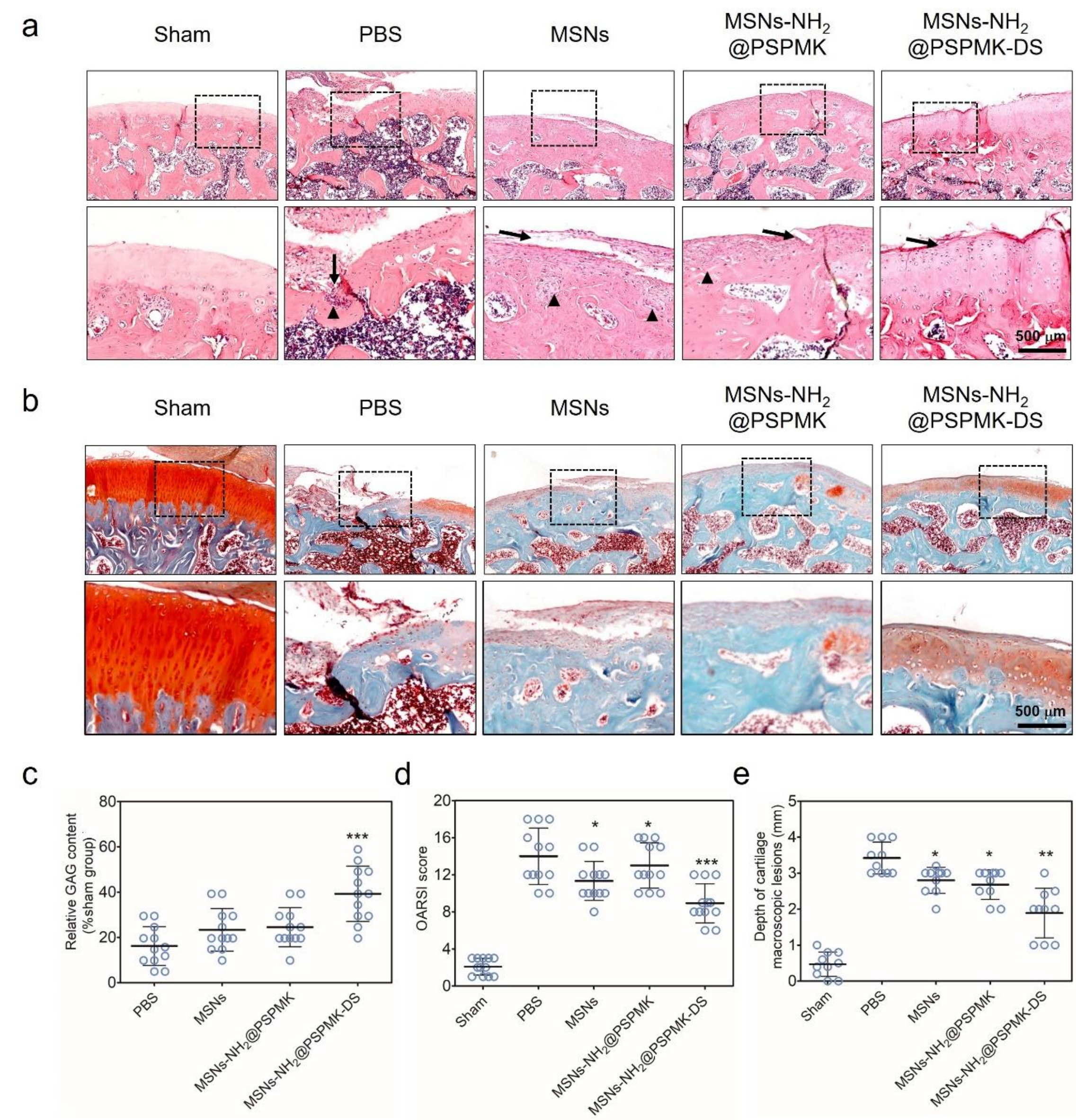

Figure 7. (a and b) Representative H&E staining (a) and Safranin O-fast green staining (b) of the cartilage sections after treatment of rat DMM-induced osteoarthritis employing PBS, MSNs, MSNs-NH_2@PSPMK and MSNs-NH_2@PSPMK-DS at eight weeks after surgery. Extensive morphological and cellular changes in the PBS group are reflected by surface irregularities and fissures (black arrows), increase in tissue cellularity with cloning (black

triangles), along with full-depth erosion and widespread cell loss. The $MSNs-NH_2$@PSPMK-DS group presents the best result in maintaining columnar architecture of normal cartilage. (c) Glycosaminoglycan (GAG) content relative to the sham group obtained from the quantification of Safranin O-fast green staining of the cartilage sections using the Image J software. The values are presented as mean ± SD, n = 12. (d) OARSI score of articular cartilage for each group after treatment for eight weeks. The values are presented as mean ± SD, n = 12. (e) Depth of cartilage macroscopic lesion for each group after treatment for eight weeks. The values are presented as mean ± SD, n = 10. *$P < 0.05$, **$P<0.01$, ***$P < 0.001$, compared with the PBS group. The results of (c-e) indicate that the $MSNs-NH_2$@PSPMK-DS group with enhanced lubrication and sustained drug release, which is bioinspired by the structure of fresh *euryale ferox* seed, demonstrates the best therapeutic effect in the treatment of osteoarthritis based on the rat DMM model.

3. Conclusions

In the present study, inspired by the fresh *euryale ferox* seed, we introduced a facile and low-toxic photopolymerization method and successfully synthesized PSPMK polymer brushes-grafted MSNs ($MSNs-NH_2$@PSPMK), which with a controllable state of the polymer chains, acted as novel nanoparticles for efficient lubrication and sustained drug release. Such nanoparticles were then encapsulated with DS to prepare the super-lubricated drug-loaded nanoparticles, $MSNs-NH_2$@PSPMK-DS, for the treatment of osteoarthritis. The lubrication and drug release tests revealed that the lubrication capability of the developed nanoparticles could be improved, while the drug release rate be sustained with the increase in the thickness of the PSPMK polymer layer. The *in vitro* and *in vivo* experiments showed that the super-lubricated drug-loaded nanoparticles with excellent biocompatibility not only protected the chondrocytes from oxidative stress-induced degeneration, but also provided therapeutic effect against development of osteoarthritis based on a rat DMM model. Combing the advantage of both efficient lubrication capability and drug loading and release behavior, the super-lubricated drug-loaded nanoparticles, MSNs-NH_2@PSPMK-DS, developed here are considered to have great potential for various biomedical applications, particularly in the situations where these two typical features are preferably desirable, for example, the treatment of osteoarthritis.

4. Experimental Section

Preparation of MSNs and MSNs-NH_2: MSNs were prepared with reference to our previous studies.[28-31] Briefly, 0.5 g of cetyltrimethyl ammonium bromide (CTAB, 98%) and 1.75 mL of NaOH solution (2 M) were added to 240 mL of aqueous solution under stirring. Afterward, 5 mL of tetraethyl orthosilicate (TEOS, 98%) was added, and then the solution was vigorously stirred at 80 °C for 15 min, followed by normal stirring for 6 h. The solution was filtered and washed with deionized water and methanol, and the CTAB template was extracted by stirring in 50 mL of methanol and 5 mL of concentrated hydrochloric acid at 60 °C for 24 h. The final resulting product (MSNs) was filtered and washed with methanol and dried under vacuum.

In order to prepare amino MSNs (MSNs-NH_2), 500 mg of MSNs was dispersed in 50 mL of anhydrous toluene, and 5 mL of 3-aminopropyltriethoxysilane (APTES, 98%) was added. The solution was refluxed under a nitrogen atmosphere for 24 h. The resulting product ($MSNs-NH_2$) was collected through centrifugation (8000 rpm, 10 min), washed twice with toluene and ethanol and dried under vacuum.

Synthesis of photopolymerization initiator: Photopolymerization initiator was synthesized following the previously published protocol.[32] 2-hydroxy-1-[4-(2-hydroxyethoxy)phenyl]-2-methyl-1-propanone (Irgacure 2959, 26.9 g, 0.12 mol), p-methyl benzene sulfonic chloride (TsCl, 19.0 g, 0.10 mol) and KOH (22.4 g, 0.40 mol) were dissolved in 300 mL of CH_2Cl_2 in a three-necked round bottom flask. The solution was stirred at room temperature for 2 h and then washed three times with deionized water. The organic layer was dried over Na_2SO_4 and distilled under vacuum. The resulting product was purified using silica gel (200~300 mesh) column chromatography, with ethyl acetate and methylene chloride (1:4, v/v) as an elution. The final product was named as 2959-Tos.

Immobilization of 2959-Tos onto $MSNs-NH_2$: Briefly, 2959-Tos (1 g), $MSNs-NH_2$ (400 mg) and K_2CO_3 (2 g) were dissolved in 30 mL of N,N-dimethylformamide (DMF, 99%) in a 50 mL round bottom flask. The solution was stirred at 110 °C for 24 h. The resulting product ($MSNs-NH_2$@I2959) was collected by centrifugation (8000 rpm, 15 min), washed with DMF and deionized water for several times, and finally dried under vacuum at room temperature overnight.

Synthesis of $MSNs-NH_2$@PSPMK: $MSNs-NH_2$@I2959 (100 mg) and SPMK monomer (1.25 mmol, 2.50 mmol, and 5.00 mmol) were dispersed in 10 mL of deionized water in a 50 mL round bottom flask. The mixture was deoxygenated by bubbling nitrogen for 30 min, and then photopolymerization was processed at 80 °C under UV-irradiation with an intensity of 5 mW/cm^2 for 90 min. The resulting product (MSNs-NH_2@PSPMK) was collected through centrifugation, washed with ethanol/H_2O (1:1, v/v) for several times, and finally dried under vacuum overnight. The product was distinguished by the monomer concentration used during the photopolymerization reaction, i.e., MSNs-NH_2@PSPMK-0.125 (0.125 M SPMK), MSNs-NH_2@PSPMK-0.250 (0.250 M SPMK) and MSNs-NH_2@PSPMK-0.500 (0.500 M SPMK).

Characterization: FTIR spectrum was recorded employing a Nicolet 6700 transform infrared spectrometer (Thermo Scientific, USA) at a wavelength ranging from 400 cm^{-1} to 4000 cm^{-1}. XPS spectrum was recorded using a 250XI XPS system (Thermo Scientific, USA), and the binding energy data were calibrated against O1s peak at 523 eV. TGA was performed on a Q5000IR instrument (TA Instruments, USA). Field emission TEM (FEI, JEM-2100F, JEOL, Japan) was used to observe the morphologies of MSNs and MSNs-NH_2@PSPMK. BET model was used to calculate specific surface area and pore volume of MSNs and MSNs-NH_2@PSPMK on the basis of the adsorption data obtained by a NOVA4000 nitrogen adsorption instrument (Quantachrome Instruments, USA). Small angle XRD measurement was performed using a diffractometer (D8, Bruker, USA) over a 2θ range from 0.6 ° to 10 ° at a scanning speed of 1 °/min.

Lubrication property: The tribological experiment was performed employing a universal material tester (UMT-3, Centre for Tribology Inc., Campbell, California, USA). All the tests were done in a reciprocating mode (oscillation amplitude: 4 mm; reciprocating frequency: 1

Hz, 3 Hz and 5 Hz) for a duration of 40 min, and the loading force was set at 1 N, 2 N and 5 N. A polished Ti6Al4V disk with a surface roughness of 1.7 nm was employed as the lower specimen, and a polyethylene (PE) ball (diameter: 8 mm) was used as the upper specimen. Here, Ti6Al4V disk and PE ball were chosen as the specimens as they have been considered to represent the most typical biomaterials for total joint replacement prosthesis, and consequently can be used to mimic physiological conditions in the joint. Different concentrations (1 mg mL^{-1}, 2 mg mL^{-1} and 5 mg mL^{-1}) of MSNs or MSNs-NH_2@PSPMK aqueous suspension were added between the two contacting pairs as the lubricant. The apparent maximum contact pressure was calculated using the Hertz equation based on the ball-on-flat configuration from our previous studies (Eq. 1),[33-36] where P is the apparent maximum contact pressure, F is the loading force (1 N, 2 N and 5 N), R is the radius of the PE ball (4 mm), E_1 and μ_1 are the elastic modulus and Poisson's ratio of Ti6Al4V (110 GPa, 0.3), and E_2 and μ_2 are the elastic modulus and Poisson's ratio of PE (1 GPa, 0.4). Accordingly, the apparent maximum contact pressure was calculated to be 26.0 MPa (1 N), 32.0 MPa (2 N) and 43.8 MPa (5 N), respectively.

$$\mathrm{P} = \frac{1}{\pi}\sqrt[3]{\frac{6F}{\left(\frac{1-\mu_1^2}{E_1}+\frac{1-\mu_2^2}{E_2}\right)^2 R^2}} \qquad \text{(Eq. 1)}$$

In vitro drug loading and release: In order to load the drug, MSNs (20 mg) and MSNs-NH_2@PSPMK (20 mg) were added to 10 mL of DS solution (0.5 mM) in phosphate buffer solution (PBS, pH 7.4). The nanoparticles were uniformly dispersed by ultrasound, and then the mixture was stirred for 48 h. The DS-loaded nanoparticles were collected by centrifugation, washed with deionized water for several times, and finally dried under vacuum. The amount of DS remaining in the solution was analyzed by a UV-vis spectrophotometer (UV-6100s, Metash Instruments, China) at a wavelength of 276 nm. The relationship between DS concentration in PBS and its absorbance at the wavelength of 276 nm was measured beforehand as the reference. The drug loading capacity (LC, %) and encapsulation efficiency (EE, %) were calculated by the following Eqs. (2-4):

$$LC(\%)_{MSNs}=\frac{\text{amount of loaded DS}}{\text{amount of DS-loaded MSNs}}\times 100 \quad \text{(Eq. 2)}$$

$$LC(\%)_{MSNs\text{-}NH_2@PSPMK}=\frac{\text{amount of loaded DS}}{\text{amount of DS-loaded MSNs-NH}_2\text{@PSPMK}}\times 100 \quad \text{(Eq. 3)}$$

$$EE(\%)=\frac{\text{amount of loaded DS}}{\text{amount of added DS}}\times 100 \quad \text{(Eq. 4)}$$

Subsequently, 20 mg of DS-loaded MSNs and 20 mg of DS-loaded MSNs-NH_2@PSPMK were first uniformly dispersed in 10 mL of PBS respectively, and then 2 mL of each sample was put into dialysis tubes (molecular weight cutoff: 8, 000~10, 000). The tubes were dialyzed in 20 mL of PBS at 37 °C. After a predetermined time, 2 mL of the medium was taken out from the release buffer and replaced by 2 mL of fresh PBS. Finally, the amount of DS released from DS-loaded nanoparticles was evaluated by the UV-vis spectrophotometer.

Primary rat chondrocyte isolation: Chondrocytes were isolated from the articular cartilage of rats in the knee joint as previously reported.[37] The articular cartilage tissues were cut into small pieces (1 mm^3) and digested with 0.25% trypsin for 30 min, followed by digestion with 0.2% type II collagenase for 4 h. The released cells were then cultured in DMEM/F12 media supplemented with 10% fetal bovine serum and antibiotics. Only the cells with less than three passages were used in this study in order to preserve chondrocyte phenotype. Unless otherwise explained, the MSNs-NH_2@PSPMK and MSNs-NH_2@PSPMK-DS used in the following tests were prepared with the SPMK monomer concentration of 0.250 M.

Cell cytotoxicity: The primary rat chondrocytes were seeded in 24-well plates with a cell density of 5×10^4/mL. The plates were incubated in a humidified atmosphere at 37 °C and 5% CO_2, and the culture medium of the plates was replaced every other day. After treatment with 1 mg mL^{-1} of MSNs, MSNs-NH_2@PSPMK and MSNs-NH_2@PSPMK-DS in triplicate for 1, 3 and 5 days, the Cell Counting Kit-8 (CCK-8, Dojindo Kagaku, Japan) was used to investigate the cytotoxicity of the nanoparticles on chondrocytes. Briefly, 0.5 mL of fresh culture medium and 50 µL of CCK-8 solution were added to each well of the plates. After incubation for 2 h, the mixed medium was transferred to 96-well plates in the darkness. The absorbance of the solution was measured employing a microplate reader (Infinite F50, Tecan, Switzerland) at a wavelength of 450 nm.

Live/Dead staining: The cell viability of the nanoparticles was analyzed by a Live/Dead Cell kit (Life Tech, USA). Chondrocytes were seeded and cultured the same as before. After being co-cultured with 1 mg mL^{-1} of MSNs, MSNs-NH_2@PSPMK and MSNs-NH_2@PSPMK-DS in triplicate for 1, 3 and 5 days, the cells were stained with 500 µL of Live/Dead cell dye for 15 min, and observed employing a fluorescence microscopy (ZEISS, Axio Imager M1, Germany). As described in the manufacturer's protocol, the viable cells with esterase activity appeared green, whereas the dead cells with compromised plasma membranes appeared red.

qRT-PCR analysis: The primary rat chondrocytes were seeded in 6-well plates with a cell density of 5×10^5/mL, treated with 10 mU of H_2O_2 and co-cultured with 1 mg mL^{-1} of MSNs, MSNs-NH$_2$@PSPMK and MSNs-NH$_2$@PSPMK-DS for 24 h. Total RNA from chondrocytes was extracted using TRIzol reagent (Invitrogen, USA) based on previously reported study.[38] The concentration and purity of the RNA preparations were determined through measuring the absorbance of RNA at 260 nm and 280 nm. cDNA was synthesized using 1 µg of RNA and a RevertAid First Strand cDNA Synthesis Kit (TaKaRa, Dalian, China). Quantitative real-time polymerase chain reaction (qRT-PCR) was performed to amplify the cDNA employing the SYBR Premix Ex Tag Kit (TaKaRa) and an ABI 7500 sequencing detection system (Applied Biosystems, Foster City, CA, USA). The mRNA levels of collagen II (Col2α), aggrecan and GAPDH were quantified by using specific primers and normalized to GAPDH. The primer sequences used in the present study were as follows: GAPDH: forward, 5‘-GAAGGTCGGTGTGAACGGATTTG-3’; reverse, 5’-CATGTAGACCATGTAGTTGAGGTCA-3’; Col2α: forward, 5’-CTCAAGTCGCTGAACAACCA-3’; reverse, 5’-GTCTCCGCTCTTCCACTCTG-3’; aggrecan: forward, 5'-GATCTCAGTGGGCAACCTTC-3'; reverse, 5’-TCCACAAACGTAATGCCAGA-3’.

Immunofluorescence staining: The chondrocytes were seeded onto sterile cover slips at a density of 5×10^4 cells per well in 24-well culture plates, treated with 10 mU of H_2O_2 and co-cultured with 1 mg mL^{-1} of MSNs, MSNs-NH$_2$@PSPMK and MSNs-NH$_2$@PSPMK-DS. After incubation for 12 h, the cells were fixed in 4% paraformaldehyde for 10 min, treated with 0.1% Triton X-100 for 15 min and incubated in 3% bovine serum albumin (BSA)/PBS for 30 min at room temperature. Afterward, the cells were incubated with rat anti-Col2α antibody (1:200 dilution) at 4 °C overnight. Following primary antibody incubation, the cells were washed employing PBS and incubated with appropriate Alexa Fluor-coupled secondary antibodies (Molecular Probes, Life Tech, USA, 1:400) for 1 h at room temperature. The cell nuclei were counterstained with 4, 6-Diamidino-2-phenyindole dilactate (DAPI, Life Tech, USA) at room temperature for 15 min in the darkness. Additionally, the cell actin was labeled with Alexa Fluor 594 phalloidin (Life Tech, USA). The images were acquired using a laser scanning confocal microscopy (LSCM, LSM800, ZEISS, Germany).

Rat osteoarthritis model and surgical procedure: This animal experiment was approved by the Animal Research Committee of Ruijin Hospital, School of Medicine, Shanghai Jiaotong University, China, which was in compliance with the National Institutes of Health Guidelines for the Care and Use of Laboratory Animals. An osteoarthritis model was established via DMM surgery in male Sprague-Dawley rats (12 weeks old; n = 25; mean body weight: 256.7 g). After the rats were anesthetized by intraperitoneal injection of pentobarbital sodium (30 mg kg^{-1} body weight), the right knee joint was exposed following a medical capsular incision and gentle lateral displacement of the extensor muscles without transection of the patellar ligament. Afterward, the medial meniscus ligament (MMTL) was transected and then the medial meniscus could be removed medially. The medial capsular incision was well sutured after restoring the extensor muscles. Additionally, a sham operation was performed employing the same approach without MMTL transection. The rats were then permitted unrestricted activity and provided free access to food and water. One week after the surgical operation, the rats were randomly sorted into five groups (n = 5 for each group) and intra-articularly injected once every week with the following formulations, i.e. PBS, MSNs,

MSNs-NH_2@PSPMK and MSNs-NH_2@PSPMK-DS. Subsequently, the rats started a running exercise on a level treadmill at a speed of 60 km/h for 1 h every other day in order to induce osteoarthritis at the knee joint.

X-ray radiograph and histological staining analyses: At one and eight weeks after surgery, the rats were scanned using an X-ray imager for small animals (Faxitron X-ray, USA) with the voltage of 32 kV and the exposure time of 6 mAs. After scanning, the rats were sacrificed and their knee joints were fixed in 4% paraformaldehyde for 24 h and decalcified in 10% EDTA. The macroscopic cartilage lesion depth for each group was measured by a vernier caliper. Afterward, the samples were dehydrated and embedded within paraffin, and then serial paraffin sections with a thickness of 5 μm were prepared and stained alternately with hematoxylin-eosin (H&E) and safranin O-fast green. The safranin O-fast green sections were evaluated utilizing the Osteoarthritis Research Society International (OARSI) score established by Pritzker *et al.*,[39] which scored the product of six grades (depth of lesion) and four stages (extent of involvement) on a scale of 0 (normal) to 24 (severe osteoarthritis). Digital images were captured and two authors (Yan and Qi) graded the sections independently. The relative glycosaminoglycan content was also measured based on the safranin O staining using Image J software.

Statistical analysis: The data were shown as mean ± standard deviation (SD), and similar independent experiments were repeated at least three times with three replicates to verify the results. One-way analysis of variance (ANOVA) was used for the multiple comparison tests. A two-tailed non-paired Student's t-test was employed to compare the significant differences between two groups, and statistical significance was displayed as *P <

0.05, **P < 0.01 or ***P < 0.001; #P < 0.05, ##P < 0.01 or ###P < 0.001.

Acknowledgements

Y. Yan, T. Sun and H. Zhang contributed equally to this work. This study was financially supported by National Key Research and Development Program of China (2018YFC1106200 and 2018YFC1106204), National Natural Science Foundation of China (51675296, 51873107 and 81572099), Ng Teng Fong Charitable Foundation (202-276-132-13), Research Fund of State Key Laboratory of Tribology, Tsinghua University, China (SKLT2018B08), Shanghai Science and Technology Commission (18ZR1434200 and 17140900102), Shanghai Municipal Education Commission—Gaofeng Clinical Medicine Grant Support (20171906) and Major Program for the Fundamental Research of Shanghai (2014ZYJB0302). Prof. H. Zhang acknowledges financial support from Jane and Aatos Erkko Foundation (grant no. 4704010), Academy of Finland (grant no. 297580) and Sigrid Jusélius Foundation (decision no. 28001830K1). Prof. H. A. Santos acknowledges financial support from the HiLIFE Research Funds and the Sigrid Jusélius Foundation (decision no. 4704580).

Received: ((will be filled in by the editorial staff))
Revised: ((will be filled in by the editorial staff))
Published online: ((will be filled in by the editorial staff))

References

[1] G. Liu, M. Cai, F. Zhou, W. Liu, *J. Phys. Chem. B* **2014**, 118, 4920.
[2] T. Sun, Y. L. Sun, H. Y. Zhang, *Polymers* **2018**, 10, 513.
[3] S. N. Jha, R. P. Kachru, *J. Food Process Eng.* **1998**, 21, 301.
[4] M. Shankar, N. Chaudhary, D. Singh, *Int. J. Pharm. Biol. Arch.* **2010**, 1, 101-107.
[5] Q. Zhang, F. Liu, K. T. Nguyen, X. Ma, X. Wang, B. Xing, Y. Zhao, *Adv. Funct. Mater.* **2012**, 22, 5144.
[6] L. He, Y. Huang, H. Zhu, G. Pang, W. Zheng, Y. S. Wong, T. Chen, *Adv. Funct. Mater.* **2014**, 24, 2754.
[7] C. de la Torre, I. Casanova, G. Acosta, C. Coll, M. J. Moreno, F. Albericio, E. Aznar, R.

Mangues, M. Royo, F. Sancenón, R. Martínez-Máñez, *Adv. Funct. Mater.* **2015**, 25, 687.
[8] L. Palanikumar, E. S. Choi, J. Y. Cheon, S. H. Joo, J. H. Ryu, *Adv. Funct. Mater.* **2015**, 25, 957.
[9] W. Ngamcherdtrakul, J. Morry, S. Gu, D. J. Castro, S. M. Goodyear, T. Sangvanich, M. M. Reda, R. Lee, S. A. Mihelic, B. L. Beckman, Z. Hu, J. W. Gray, W. Yantasee, *Adv. Funct. Mater.* **2015**, 25, 2646.
[10] Z. Li, J. Barnes, A. Bosoy, J. F. Stoddart, J. Zink, *Chem. Soc. Rev.* **2012**, 41, 2590.
[11] Y. L. Sun, H. Y. Zhang, Y. X. Wang, Y. Wang, *J. Con. Rel.* **2017**, 259, 45.
[12] Y. Sun, Y. Yang, *J. Con. Rel.* **2013**, 8, 181.
[13] Z. Qu, H. Xu, H. Gu, *ACS Appl. Mater. Interfaces* **2015**, 7, 14537.
[14] T. Ribeiro, E. Coutinho, A. S. Rodrigues, C. Baleizão, J. P. S. Farinha, *Nanoscale* **2017**, 9, 13485.
[15] D. R. Radu, C. Y. Lai, J. W. Wiench, M. Pruski, V. S. Lin, *JACS* **2004**, 126, 1640.
[16] C. Boyer, N. A. Corrigan, K. Jung, D. Nguyen, T. K. Nguyen, N. M. Adnan, S. Oliver, S. Shanmugam, J. Yeow, *Chem. Rev.* **2016**, 116, 1803.
[17] J. Klein, *Science* **2009**, 323, 47.
[18] S. Jahn, J. Seror, J. Klein, *Annu. Rev. Biomed. Eng.* **2016**, 18, 235.
[19] J. Klein, *Friction* **2013**, 1, 1.
[20] J. Seror, L. Zhu, R. Goldberg, A. J. Day, J. Klein, *Nat Commun.* **2015**, 6, 6497.
[21] M. Kobayashi, A. Takahara, *Chem. Rec.* **2010**, 10, 208.
[22] J. Seror, Y. Merkher, N. Kampf, L. Collinson, A. J. Day, A. Maroudas, J. Klein, *Biomacromolecules* **2011**, 12, 3432.
[23] G. Liu, Z. Liu, N. Li, X. Wang, F. Zhou, W. Liu, *ACS Appl. Mater. Interfaces* **2014**, 22, 20452.
[24] M. Kobayashi, M. Terada, A. Takahara, *Faraday Discuss* **2012**, 156, 403.
[25] X. Zhu, C. Yan, F. M. Winnik, D. Leckband, *Langmuir* **2007**, 23, 162.
[26] J. Israelachvili, Intermolecular and surface forces, 2nd ed.; Academic Press: San Diego, CA, 1991.
[27] H. Iijima, T. Aoyama, A. Ito, J. Tajino, M. Nagai, X. Zhang, S. Yamaguchi, H. Akiyama, H. Kuroki, *Osteoarthr Cartilage* **2014**, 22, 1036.
[28] Y. Sun, B. Yang, S. X. Zhang, Y. Yang, *Chem. Eur. J.* **2012**, 18, 9212.
[29] Y. Sun, Y. Yang, D. Chen, G. Wang, Y. Zhou, C. Wang, J.F. Stoddart, *Small* **2013**, 9, 3224.
[30] H. Y. Zhang, Y. F. Sun, Y. L. Sun, M. Zhou, *Bio-Med. Mater. Eng.* **2014**, 24, 2211.
[31] Y. Wang, W. G. Cui, X. Zhao, S. Z. Wen, Y. L. Sun, J. M. Han, H. Y. Zhang, *Nanoscale*, **2018**, DOI: 10.1039/C8NR07329E.
[32] F. Sun, Y. Li, N. Zhang, J. Nie, *Polymers* **2014**, 55, 3656.
[33] H. Y. Zhang, J. B. Luo, M. Zhou, Y. Zhang, Y. L. Huang, *J. Mech. Beh. Biomed. Mater.* **2013**, 20, 209.
[34] H. Y. Zhang, S. H. Zhang, J. B. Luo, Y. H. Liu, S. H. Qian, F. H. Liang, Y. L. Huang, *J. Tribology, Transactions of ASME* **2013**, 135, 032301.
[35] H. Y. Zhang, Y. J. Zhu, X. Y. Hu, Y. F. Sun, Y. L. Sun, J. M. Han, Y. Yan, M. Zhou, *Bio-Med. Mater. Eng.* **2014**, 24, 2151.
[36] Y. Y. Jiao, S. Z. Liu, Y. L. Sun, W. Yue, H. Y. Zhang, *Langmuir*, **2018**, DOI:

10.1021/acs.langmuir.8b02441.
[37] A. Mirando, Y. Dong, J. Kim, *Methods Mol. Biol.* **2014**, 1130, 267.
[38] C. Li, K. Chen, H. Kang, *Cell Death Dis.* **2017**, 8, 3165.
[39] K. P. H. Pritzker, S. Gay, S. A. Jimenez, K. Ostergaard, J. P. Pelletier, P. A. Revell, D. Salter, W. B. van den Berg, *Osteoarthr Cartilage* **2006**, 14, 13.

Graphical Abstract

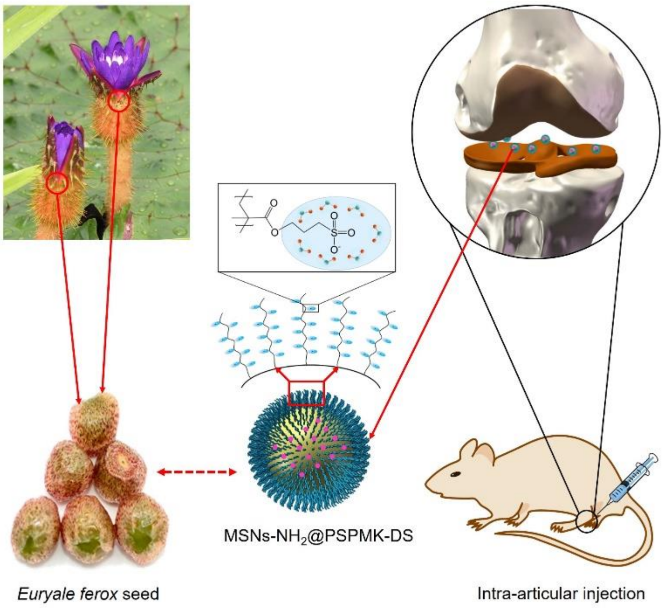

Bioinspired by the unique structure of fresh *euryale ferox* seed, a novel super-lubricated drug-loaded nanoparticle was designed and synthesized based on photopolymerization for treatment of osteoarthritis.

Scheme 1

Click here to access/download
Production Data
Scheme 1.tif

Figure 1

Click here to access/download
Production Data
Figure 1.tif

Figure 2

Click here to access/download
Production Data
Figure 2.tif

Figure 3

Click here to access/download
Production Data
Figure 3.tif

Figure 4

Click here to access/download
Production Data
Figure 4.tif

Figure 5

Click here to access/download
Production Data
Figure 5.tif

Figure 6

Click here to access/download
Production Data
Figure 6.tif

Figure 1

Click here to access/download
Production Data
Figure 7.tif

ToC

Click here to access/download
Production Data
Graphic abstract.tif